

15

Non-linear Waves, Shocks and Solitons

Non-linear Effects in Acoustic Waves

The linearity of the longitudinal acoustic waves discussed in Chapter 6 required the assumption of a constant bulk modulus

$$B = -\frac{dP}{dV/V}$$

If the amplitude of the sound wave is too large this assumption is no longer valid and the wave propagation assumes a new form. A given mass of gas undergoing an adiabatic change obeys the relation

$$\frac{P}{P_0} = \left(\frac{V_0}{V}\right)^\gamma = \left[\frac{V_0}{V_0(1+\delta)}\right]^\gamma$$

in the notation of Chapter 6, so that

$$\frac{\partial P}{\partial x} = \frac{\partial p}{\partial x} = -\gamma P_0(1+\delta)^{-(\gamma+1)} \frac{\partial^2 \eta}{\partial x^2}$$

since $\delta = \partial\eta/\partial x$.

Since $(1+\delta)(1+s) = 1$, we may write

$$\frac{\partial p}{\partial x} = -\gamma P_0(1+s)^{\gamma+1} \frac{\partial^2 \eta}{\partial x^2}$$

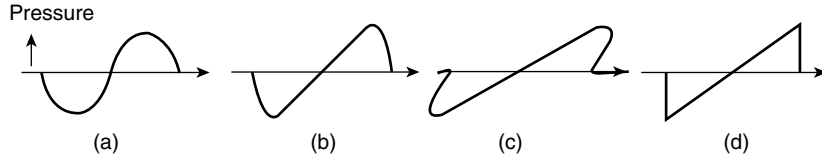


Figure 15.1 The local sound velocity in a high amplitude acoustic wave (a) is pressure and density dependent. The wave distorts with time (b) as the crest overtakes the lower density regions. The extreme situation of (c) is prevented by entropy-producing mechanisms and the wave stabilises to an N type shock-wave (d) with a sharp leading edge

and from Newton's second law we have

$$\frac{\partial p}{\partial x} = -\rho_0 \frac{\partial^2 \eta}{\partial t^2}$$

so that

$$\frac{\partial^2 \eta}{\partial t^2} = c_0^2 (1 + s)^{\gamma+1} \frac{\partial^2 \eta}{\partial x^2}, \quad \text{where} \quad c_0^2 = \frac{\gamma P_0}{\rho_0} \quad (15.1)$$

Physically this implies that the local velocity of sound, $c_0(1 + s)^{(\gamma+1)/2}$, depends upon the condensation s , so that in a finite amplitude sound wave regions of higher density and pressure will have a greater sound velocity, and local disturbances in these parts of the wave will overtake those where the values of density pressure and temperature are lower.

A single sine wave of high amplitude can be formed by a close fitting piston in a tube which is pushed forward rapidly and then returned to its original position. Figure 15.1a shows the original shape of such a wave and 15.1b shows the distortion which follows as it propagates down the tube. If the distortion continued the wave form would eventually appear as in Figure 15.1c, where analytical solutions for pressure, density and temperature would be multi valued, as in the case of the non-linear oscillator of Figure 14.3c. Before this situation is reached, however, the wave form stabilizes into that of Figure 15.1d, where at the vertical 'shock front' the rapid changes of particle density, velocity and temperature produce the dissipating processes of diffusion, viscosity and thermal conductivity. The velocity of this 'shock front' is always greater than the velocity of sound in the gas into which it is moving, and across the 'shock front' there is always an increase in entropy. The competing effects of dissipation and non-linearity produce a stable front as long as the wave retains sufficient energy. The N -type wave of Figure 15.1d occurs naturally in explosions (in spherical dimensions) where a blast is often followed by a rarefaction.

The growth of a shock front may also be seen as an extension of the Doppler effect (p. 141), where the velocity of the moving source is now greater than that of the signal. In Figure 15.2a as an aircraft moves from S to S' in a time t the air around it is displaced and the disturbance moves away with the local velocity of sound v_s . The circles show the positions at time t of the sound wave fronts generated at various points along the path of the aircraft but if the speed of the aircraft u is greater than the velocity of sound v_s regions of high density and pressure will develop, notably at the edges of the aircraft structure and

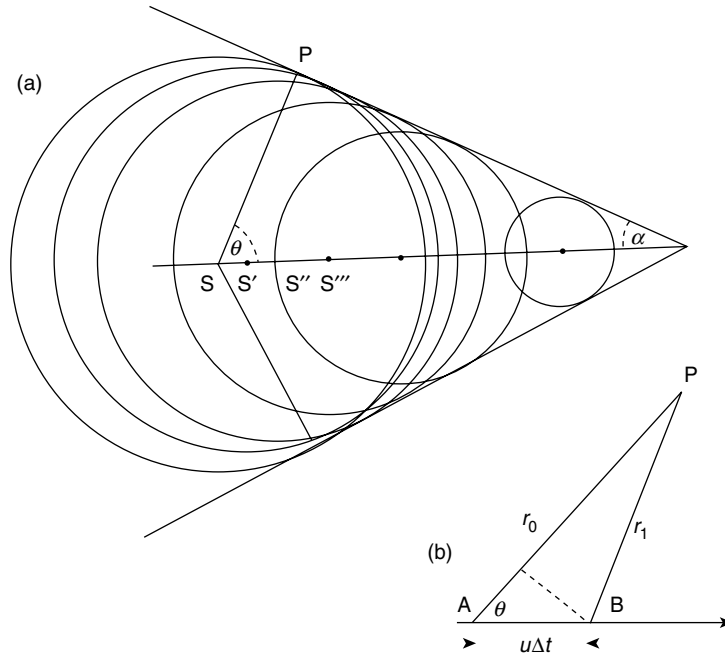


Figure 15.2 (a) The circles are the wavefronts generated at points S along the path of the aircraft, velocity $u > v_S$ the velocity of sound. Wavefronts superpose on the surface of the Mach Cone (typical point P) of half angle $\alpha = \sin^{-1} v_S/u$ to form a shock front. (b) At point P sound waves arrive simultaneously from positions A and B along the aircraft path when $(u/v_S) \cos \theta = 1$. ($\theta + \alpha = 90^\circ$)

along the conical surface tangent to the successive wavefronts which are generated at a speed greater than sound and which build up to a high amplitude to form a shock. The cone, whose axis is the aircraft path, has half angle α where

$$\sin \alpha = \frac{v_S}{u}$$

It is known as the ‘Mach Cone’ and when it reaches the ground a ‘supersonic bang’ is heard.

The growth of the shock at the surface of the cone may be seen by considering the sound waves in Figure 15.2(b) generated at points A (time t_A) and B (time t_B) along the path of the aircraft, which travels the distance $AB = x = u\Delta t$ in the time interval $\Delta t = t_B - t_A$. The sound waves from A will travel the distance r_0 to reach the point P at a time

$$t_0 = t_A + \frac{r_0}{v_S}$$

Those from B will travel the distance r_1 to P to arrive at a time

$$t_1 = t_B + \frac{r_1}{v_S}$$

If x is small relative to r_0 and r_1 , we see that

$$r_1 - r_0 \approx x \cos \theta = u \Delta t \cos \theta$$

so the time interval

$$\begin{aligned} t_1 - t_0 &= t_B - t_A + \frac{(r_1 - r_0)}{v_S} \\ &= \Delta t - \frac{u \Delta t \cos \theta}{v_S} = \Delta t \left(1 - \frac{u \cos \theta}{v_S} \right) \end{aligned}$$

For the aircraft speed $u < v_S$, $t_1 - t_0$ is always positive and the sound waves arrive at P in the order in which they were generated.

For $u > v_S$ this time sequence depends on θ and when

$$\frac{u}{v_S} \cos \theta = 1$$

$t_1 = t_0$ and the sound waves arrive simultaneously at P to build up a shock.

Now the angles θ and α are complementary so the condition

$$\cos \theta = \frac{v_S}{u}$$

defines

$$\sin \alpha = \frac{v_S}{u}$$

so that all points P lie on the surface of the Mach Cone.

A similar situation may arise when a charged particle q emitting electromagnetic waves moves in a medium of refractive index greater than unity with a velocity v_q which may be greater than that of the phase velocity v of the electromagnetic waves in the medium ($v < c$). A Mach Cone for electromagnetic waves is formed with a half angle α where

$$\sin \alpha = \frac{v}{v_q}$$

And the resulting 'shock wave' is called Cerenkov radiation. Measuring the effective direction of propagation of the Cerenkov radiation is one way of finding the velocity of the charged particle.

Shock Front Thickness

The extent of the region over which the gas properties change, the shock front thickness, may be only a few mean free paths in a monatomic gas because only a few collisions between atoms are necessary to exchange the energy required to raise them from the

equilibrium conditions ahead of the shock to those behind it. In a polyatomic gas the collisions are effective in producing a rapid increase in translational and rotational mode energies, but vibrational modes take much longer to reach their new equilibrium, so that the shock front thickness is very much greater.

Within the shock front thickness the state of the gas is not easily found, but the state of the gas on one side of the shock may be calculated from the state of the gas on the other side by means of the conservation equations of mass, momentum and energy.

Equations of Conservation

In a laboratory, shock waves are produced in a tube which is divided by a diaphragm into a short high-pressure section and a much longer low-pressure section. When the diaphragm bursts the expanding high pressure gas behaves as a very fast low-inertia piston which compresses the low pressure gas on the other side of the diaphragm and drives a shock wave down the tube. The profile of this shock wave is the step function shown as the dotted line in Figure 15.3, and the gas into which the shock is propagating is considered to be at rest. This simplifies the analysis, for we can consider the situation in Figure 15.3 as it appears to an observer O travelling with the shock front velocity u_1 into the stationary gas. The shock front is located within the region bounded by the surfaces A and B of unit area, each of which remains fixed with respect to the observer. The stationary gas which moves through the shock front from surface B acquires a flow velocity $u < u_1$ and a velocity relative to the shock front of $u_2 = u_1 - u$. From the observer's viewpoint the quantity of gas flowing into unit area of the region AB per unit time is $\rho_1 u_1$, where ρ_1 is the density of

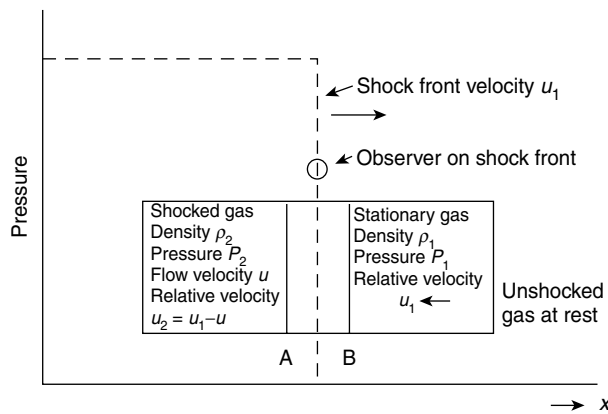


Figure 15.3 The pressure 'step profile' of a shock wave developed in a shock tube is shown by the dotted line. The plane cross-sections at A and B remain fixed with respect to the observer O moving with the shock front at velocity u_1 into unshocked gas at rest of pressure p_1 and density ρ_1 . The shocked gas has a pressure p_2 , a density ρ_2 and a velocity u , with a relative velocity $u_2 = u_1 - u$ with respect to the shock front. The states of the gas at A and B are related by the conservation equations of mass, momentum and energy across the shock front. Experimental measurement of the shock velocity u_1 is sufficient to determine the unknown parameters if the stationary gas parameters are known

the gas ahead of the shock. The quantity leaving unit area of AB per unit time is $\rho_2(u_1 - u) = \rho_2 u_2$, where ρ_2 is the density of the shocked gas.

Conservation of mass yields $\rho_1 u_1 = \rho_2 u_2 = m$ (a constant mass). The force per unit area acting across the region AB is $p_2 - p_1$, which equals the rate of change of momentum of the gas within the unit element, which is $m(u_1 - u_2)$. The conservation of momentum is therefore given by

$$p_1 + \rho_1 u_1^2 = p_2 + \rho_2 u_2^2.$$

The work done on unit area of the region per unit time is $p_1 u_1 - p_2 u_2$, and this equals the rate of increase of the kinetic and internal energy of the gas passing through unit area of the shock wave.

The difference

$$p_1 u_1 - p_2 u_2 = \frac{p_1}{\rho_1} m - \frac{p_2}{\rho_2} m$$

so that if the internal energy per unit mass of the gas is written $e(p, \rho)$, then the equation of conservation of energy per unit mass becomes

$$\frac{1}{2} u_1^2 + e_1 + \frac{p_1}{\rho_1} = \frac{1}{2} u_2^2 + e_2 + \frac{p_2}{\rho_2}$$

where for an ideal gas $p/\rho = RT$ and $e = c_v T = (1/\gamma - 1)p/\rho$, where T is the absolute temperature, c_v is the specific heat per gram at constant volume and $\gamma = c_p/c_v$, where c_p is the specific heat per gram at constant pressure.

These three conservation equations

$$\rho_1 u_1 = \rho_2 u_2 = m \quad (\text{mass})$$

$$p_1 + \rho_1 u_1^2 = p_2 + \rho_2 u_2^2 \quad (\text{momentum})$$

and

$$\frac{1}{2} u_1^2 + e_1 + \frac{p_1}{\rho_1} = \frac{1}{2} u_2^2 + e_2 + \frac{p_2}{\rho_2} \quad (\text{energy})$$

together with the internal energy relation $e(p, \rho)$ completely define the properties of an ideal gas behind a shock wave in terms of the stationary gas ahead of it.

In an experiment the properties of the gas ahead of the shock are usually known, leaving five unknowns in the four equations, which are the shock front velocity u_1 , the density of the shocked gas ρ_2 , the relative flow velocity behind the shock u_2 , the shocked gas pressure p_2 and its internal energy e_2 . In practice the shock front velocity u_1 is measured and the other four properties may then be calculated.

Mach Number

A significant parameter in shock wave theory is the Mach number. It is a local parameter defined as the ratio of the flow velocity to the local velocity of sound. The Mach number of

the shock front is therefore $M_s = u_1/c_1$, where u_1 is the velocity of the shock front propagating into a gas whose velocity of sound is c_1 .

The Mach number of the gas flow behind the shock front is defined as $M_f = u/c_2$, where u is the flow velocity of the gas behind the shock front ($u < u_1$) and c_2 is the local velocity of sound behind the shock front. There is always an increase of temperature across the shock front, so that $c_2 > c_1$ and $M_s > M_f$. The physical significance of the Mach number is seen by writing $M^2 = u^2/c^2$, which indicates the ratio of the kinetic flow energy, $\frac{1}{2}u^2 \text{ mol}^{-1}$, to the thermal energy, $c^2 = \gamma RT \text{ mol}^{-1}$. The higher the proportion of the total gas energy to be found as kinetic energy of flow the greater is the Mach number.

Ratios of Gas Properties Across a Shock Front

A shock wave may be defined in terms of the shock Mach number M_s , the density or compression ratio across the shock front $\beta = \rho_2/\rho_1$, the temperature ratio across the shock T_2/T_1 and the compression ratio or shock strength $y = p_2/p_1$.

Given the shock strength, $y = p_2/p_1$, the conservation equations are easily solved to yield

$$M_s = \frac{u_1}{c_1} = \left(\frac{y + \alpha}{1 + \alpha} \right)^{1/2}$$

where

$$\alpha = \frac{\gamma - 1}{\gamma + 1}$$

$$\beta = \frac{\rho_2}{\rho_1} = \frac{\alpha + y}{1 + \alpha y}$$

and

$$\frac{T_2}{T_1} = y \left(\frac{1 + \alpha y}{\alpha + y} \right)$$

Alternatively these may be written in terms of the experimentally measured parameter M_s as

$$\frac{p_2}{p_1} = y = M_s^2(1 + \alpha) - \alpha$$

$$\frac{\rho_2}{\rho_1} = \beta = \frac{M_s^2}{1 - \alpha + \alpha M_s^2}$$

and

$$\frac{T_2}{T_1} = \frac{[\alpha(M_s^2 - 1) + M_s^2][\alpha(M_s^2 - 1) + 1]}{M_s^2}$$

For weak shocks (where p_2/p_1 is just greater than 1) β , T_2/T_1 and M_s are also just greater than unity, and the shock wave moves with the speed of sound.

Strong Shocks

The ratio $p_2/p_1 \gg 1$ defines a strong shock, in which case

$$M_s^2 \rightarrow \frac{(\gamma + 1)}{2\gamma} y$$

and

$$\beta = \frac{\rho_2}{\rho_1} \rightarrow \left(\frac{\gamma + 1}{\gamma - 1} \right)$$

a limit of 6 for air and 4 for a monatomic gas for a constant γ . The flow velocity

$$u = u_1 - u_2 \rightarrow \frac{2u_1}{(\gamma + 1)}$$

and the temperature ration

$$\frac{T_2}{T_1} = \left(\frac{c_2}{c_1} \right)^2 \rightarrow \frac{(\gamma - 1)}{(\gamma + 1)} y$$

The temperature increase across strong shocks is of great experimental interest. The physical reason for this increase may be seen by rewriting the equation of energy conservation as $\frac{1}{2}u_1^2 + h_1 = \frac{1}{2}u_2^2 + h_2$, where $h = (e + p/\rho)$ is the total heat energy or enthalpy per unit mass. For strong shocks $h_2 \gg h_1$ of the cold stationary gas and $u_1 \gg u_2$, so that the energy equation reduces to $h_2 \approx \frac{1}{2}u_1^2$, which states that the relative kinetic energy of a stationary gas element just ahead of the shock front is converted into thermal energy when the shock wave moves over that element. The energy of the gas which has been subjected to a very strong shock wave is almost equally divided between its kinetic energy and its thermal or internal energy. This may be shown by considering the initial values of the internal energy e_1 and pressure p_1 of the cold stationary gas to be negligible quantities in the conservation equations, giving the kinetic energy per unit mass behind the shock as

$$\frac{1}{2}u^2 = \frac{1}{2}(u_1 - u_2)^2 = e_2$$

the internal energy per unit mass of the shocked gas.

In principle, the temperature behind very strong shock waves should reach millions of degrees. In practice, real gas effects prevent this. In a monatomic gas high translational energies increase the temperature until ionization occurs and this process then absorbs energy which otherwise would increase the temperature still further. In a polyatomic gas the total energy is divided amongst the various modes (translational, rotational and vibrational) and the temperatures reached are much lower than in the case of the monatomic gas. The reduction of γ due to these processes is significant, since with

increasing ionization $\gamma \rightarrow 1$, and the temperature ratio depends upon the factor $(\gamma - 1)/(\gamma + 1)$ which becomes very small.

(Problems 15.1, 15.2, 15.3, 15.4, 15.5, 15.6)

Solitons

We have seen that a pulse, limited in space, is also limited in time. Fourier analysis shows that a pulse is the superposition of a large number of components with different frequencies and that the high frequency components contribute to the vertical edges of the pulse Figure 10.3. The superposition of these components changes as phase differences develop; different frequencies will have different phase velocities and the pulse disperses.

It is surprising, therefore, that high amplitude solitary waves or solitons are known to exist. The first recorded observation of a soliton is that of Scott–Russel (1844) who saw a single wave about 40 cm high travelling along a canal in Scotland. Rayleigh (1876) developed an expression for the shape of this soliton based on the hydrodynamics of waves in shallow water.

That expression, the bell-shaped Figure 15.4 is given by

$$\eta = a \operatorname{sech}^2 \alpha(x - x_0)$$

where

$$\alpha = \frac{1}{2} \sqrt{\frac{3a}{h^2(h+a)}}$$

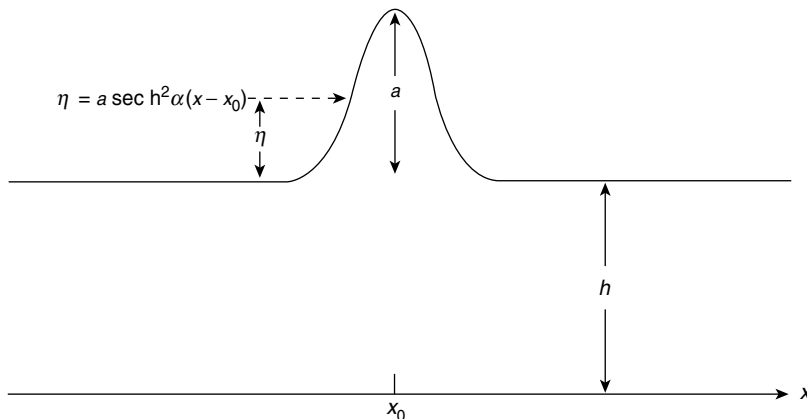


Figure 15.4 The solitary wave (soliton) on a shallow canal seen by Scott–Russel (1844) was described as a sech^2 bell-shaped function by Rayleigh (1876). The canal depth is h , the soliton amplitude is a and η measures a displacement on the soliton curve. The soliton is centred at x_0 and α is a function of a and h

η , a , h and x_0 are all shown in Figure 15.4. The coordinate x_0 about which the static figure is centred is replaced by ct when the soliton is moving; c is the soliton velocity and t is the time. We shall see that c is related to the height of the soliton. Larger amplitude solitons move faster.

Further sightings of solitons on Dutch canals led to a thorough discussion of waves with finite amplitude in shallow water by Korteweg and de Vries (1895). Their equation describing soliton behaviour is known as the KdV equation and is now taken as the basis of soliton theory. We shall not pursue the relevant fluid dynamics necessary to obtain the KdV equation but we shall obtain its mathematical form by a method which may lack formal rigour but which provides a good working model. It also emphasizes the physical characteristics which produce a soliton.

The underlying physics of solitons is the competition between two processes. One of these causes a high amplitude or non-linear wave to break; we have seen this in the formation of a shock wave in Figure 15.1c. This results from the increased phase velocities of the high amplitude non-linear components of the wave.

In a soliton this is opposed by the dispersion of the wave components in such a way that a stable profile is maintained.

We shall derive the form of the KdV equation and then discuss the following topics:

- Solitons, Schrödinger's equation and elementary particles.
- Solitons in optical fibres. Telecommunications..

A list of references is given at the end of the chapter.

Non-Linearity

Equation (15.1) shows that the higher amplitude components of an acoustic wave propagate with a phase velocity

$$v = \frac{\partial x}{\partial t} = c_0(1 + s)^{\gamma+1/2}$$

where c_0 is the phase velocity of a small amplitude linear wave and s , the condensation, is a measure of the compression in the wave.

We may expand this, to a first order, to give

$$v = \frac{\partial x}{\partial t} = c_0 \left(1 + \frac{\gamma + 1}{2} s \dots \right) \quad (15.2)$$

In a linear, low-amplitude, right-going wave we have

$$\eta = \eta_m e^{i(\omega t - kx)}$$

So, denoting $\partial\eta/\partial t$ as η_t and $\partial\eta/\partial x$ as η_x we have

$$\eta_t/\eta_x = \frac{-\omega}{k} = -c_0$$

or

$$\eta_t + c_0\eta_x = 0 \quad (15.3)$$

Throughout this chapter we shall indicate partial differentiation with respect to a variable by writing that variable as a subscript. Thus, $\eta_t = \partial\eta/\partial t$; $\eta_x = \partial\eta/\partial x$; $\eta_{tt} = \partial^2\eta/\partial t^2$ and $\eta_{xx} = \partial^2\eta/\partial x^2$. Replacing c_0 in equation (15.3) by v in equation (15.2) gives

$$\eta_t + c_0 \left[1 + \left(\frac{\gamma + 1}{2} \right) s \right] \eta_x = 0$$

which, because $s = k\eta$ is in phase with η_t (Figure 6.2), becomes

$$\eta_t + c_0 \left[1 + \left(\frac{\gamma + 1}{2} \right) k\eta \right] \eta_x = \eta_t + c_0\eta_x + c_0 \left(\frac{\gamma + 1}{2} \right) k\eta\eta_x = 0 \quad (15.4)$$

We are interested in non-linear effects and after removing the linear contribution of equation (15.4) we are left with the non-linear expression

$$\eta_t + b\eta\eta_x = 0 \quad (15.5)$$

where

$$b = c_0 \left(\frac{\gamma + 1}{2} \right) k$$

Equation (15.5) provides the first two terms of the KdV equation. We now consider the third, the dispersion term, which competes with the non-linear $b\eta\eta_x$ term.

Dispersion and the Form of the KdV Equation A typical dispersion equation is that for transverse and longitudinal waves in a periodic structure given by equation (5.12) as

$$v = \frac{\omega}{k} = c_0 \left(\frac{\sin ka/2}{ka/2} \right)$$

where k is the wave number and a is the particle separation. For small k , long λ , we may expand the sine term to give

$$v = \frac{\omega}{k} = \frac{c_0}{ka/2} \left[\frac{ka}{2} - \left(\frac{ka}{2} \right)^3 \dots + \right]$$

or

$$\omega = c_0 k \left[1 - \left(\frac{ka}{2} \right)^2 \right] = c_0 k - dk^3 \quad (15.5a)$$

where

$$d = c_0 a^2 / 4$$

Writing a linear wave in the form

$$\eta = \eta_m e^{i(\omega t - kx)}$$

gives

$$\eta_t = i\omega\eta, \quad \eta_x = -ik\eta \quad \text{and} \quad \eta_{xxx} = ik^3\eta$$

which, with equation (15.5a), gives

$$\eta_t + c_0 \eta_x + d \eta_{xxx} = 0$$

Again, the contribution $\eta_t + c_0 \eta_x$ applies only to linear waves and replacing this for non-linear waves by equation 15.5

$$\eta_t + b \eta \eta_x$$

gives

$$\eta_t + b \eta \eta_x + d \eta_{xxx} = 0 \quad (15.6)$$

where b and d are constant coefficients. This is the form of the KdV equation which describes soliton behaviour. The coefficients b and d depend upon the particular soliton under discussion.

We gain an insight into the effect of the dispersion term by considering the following. Let us write a right-going linear wave in the form

$$\eta = \eta_m e^{i(\omega t - kx)} = \eta_m e^{ik(c_0 t - x)}$$

where

$$\omega = c_0 k$$

The effect of dispersion, from the previous section, changes $\omega = c_0 k$ to

$$\omega = c_0 k \left[1 - \left(\frac{ka}{2} \right)^2 \right]$$

so we have

$$\eta = \eta_m \exp \left(ik \left[c_0 \left\{ 1 - \left(\frac{ka}{2} \right)^2 \right\} t - x \right] \right)$$

and dispersion has the effect of shifting the wave. Note that in this case of normal dispersion the shift retards the higher k , shorter wavelength terms.

Mathematically, this dispersive shift is used to offset the steepening, wave breaking effects of non-linearity. The technique, known as a Gardner–Morikawa transformation, is to choose a coordinate system which moves with the velocity c_0 , the pulse rides on this moving coordinate so that dispersion relative to c_0 is much reduced. In addition, because any dispersive change is now so much slower, a much longer time scale $\tau > t$ is chosen and the final aim is to show that changes in the soliton profile are negligible in the τ time scale.

The Elements of the KdV Equation Although we derived the form of the KdV equation using the amplitude η , the equation is most often written in terms of a quantity u which may represent any property of the wave which varies with distance and time.

In their paper ‘The Discovery of the Soliton’ (1965) Zabusky and Kruskal used the equation in the form

$$u_t + uu_x + \delta^2 u_{xxx} = 0 \quad (15.7)$$

where $\delta \ll 1$.

Their experiment was made by computer simulation. In the absence of the third dispersive term the non-linear equation

$$u_t + uu_x = 0 \quad (15.8)$$

describes the development of the shock wave of Figure 15.1. The positive pulses of Figure 15.1a, b and c are superposed in Figure 15.5 with u plotted against x . It is evident that u_t increases with higher values of u and equation (15.8) retains a single valued solution only as long as the gradient u_x of the leading edge becomes increasingly negative as the pulse steepens.

Now equation (15.8) is satisfied by any function $u = f(x - ut)$ —see Problem 15.7—and

$$u_x = (1 - u_x t) f' \quad (15.9)$$

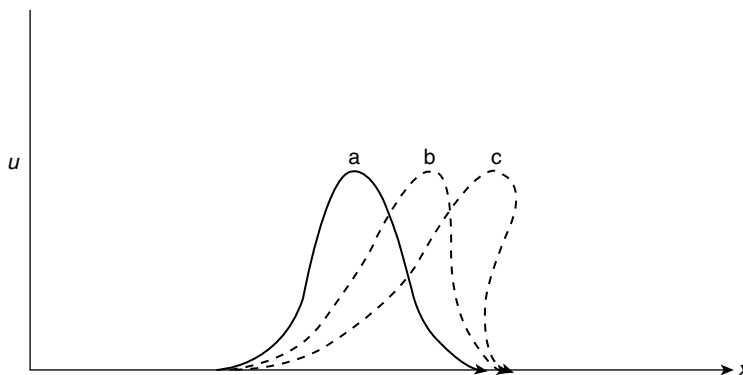


Figure 15.5 Figs. 15.1 (a), (b) and (c) superimposed to show breaking of a non-linear wave

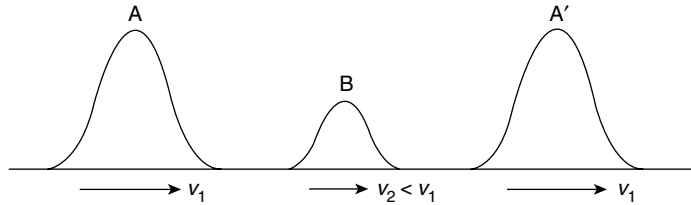


Figure 15.6 The velocity of a soliton increases with its magnitude and solitons are transparent in mutual collisions, each retaining its own identity. A large soliton A overtakes a smaller soliton B to emerge as A' with B unaffected

where

$$f' = \partial f / \partial (x - ut)$$

Taking the pulse profile at $t = 0$ as $u = f(x) = \cos \pi x$ equation (15.9) shows that $u_x = -\infty$ at $u \approx 0$ (the foot of the pulse) when $x = 0.5$ and $t = 1/\pi$. At this point the wave becomes infinitely steep and breaks. This behaviour was observed by Zabusky and Kruskal. When Zabusky and Kruskal added the third dispersion term in their computer experiment to give the KdV equation

$$u_t + uu_x + \delta^2 u_{xxx} = 0$$

they found that after a time $t = 1/\pi$ the solution broke into a train of solitary waves (solitons) of successively larger amplitudes with the larger waves travelling faster than the smaller ones. Even more important from the point of view of optical solitons, after one soliton had overtaken another, each soliton retained its unique identity (Figure 15.6). Solitons are transparent to each other and are unaffected by mutual collisions.

(Problems 15.7, 15.8)

Two Important Forms of the KdV Equation

1. The KdV equation for shallow water waves may be written in the form

$$u_t + 6uu_x + u_{xxx} = 0 \quad (15.10)$$

with a solution

$$\begin{aligned} u(x, t) &= 2\alpha^2 \operatorname{sech}^2 \alpha(x - ct) \\ &= 2 \frac{\partial^2}{\partial x^2} \log [1 + e^{2\alpha(x-ct)}] \end{aligned}$$

or

$$u(x, t) = 2 \frac{\partial^2}{\partial x^2} \log [1 + e^{-2\alpha(x-ct)}]$$

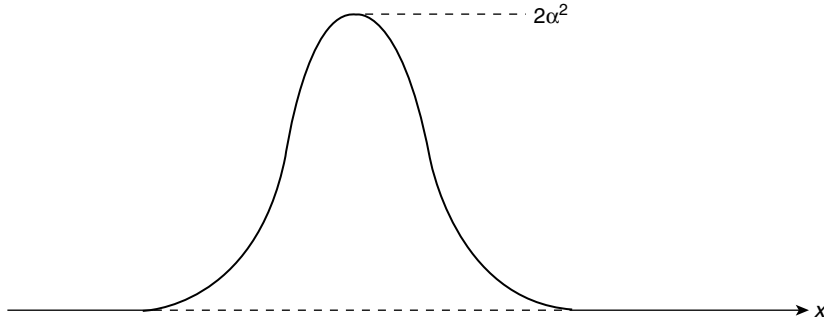


Figure 15.7 The KdV equation $u_t + 6uu_x + u_{xxx} = 0$ has a soliton solution $u(x, t) = 2\alpha^2 \operatorname{sech}^2 \alpha(x - ct)$ with a maximum value of $2\alpha^2$

Note that the exponents in the log solutions may be positive or negative.

The sech^2 form of the solution may be seen to fit equation (15.10) with a soliton velocity $c = 4\alpha^2$ (twice the maximum value of u) by showing that

$$\begin{aligned} u_t &= 2\alpha u c \tanh \phi, \quad \text{where } \phi = \alpha(x - ct) \\ uu_x &= -2\alpha u^2 \tanh \phi \end{aligned}$$

and

$$u_{xxx} = -8\alpha^3 u \tanh \phi + 12\alpha u^2 \tanh \phi$$

The sech^2 shape of the soliton is shown in Figure 15.7. Its peak value is

$$u = 2\alpha^2$$

(Problems 15.9, 15.10)

2. The second important form of the KdV equation is

$$u_t - 6uu_x + u_{xxx} = 0 \tag{15.11}$$

(the shallow water wave form with a negative second term). This has a time independent soliton solution of

$$u(x) = -2\alpha^2 \operatorname{sech}^2(x - x_0)$$

where x_0 locates the centre of the soliton. This solution may be shown to satisfy equation (15.11) by calculating u_x and u_{xxx} as for equation (15.10).

A graph of this soliton, Figure 15.8, shows its minimum to have a value of $-2\alpha^2$. Its importance is its connection with Schrödinger's equation, which we now discuss.

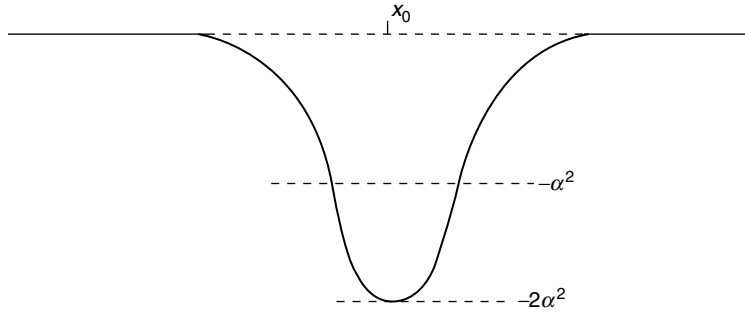


Figure 15.8 The KdV equation $u_t - 6uu_x + u_{xxx} = 0$ has a time independent solution $u(x) = -2\alpha^2 \operatorname{sech}^2 \alpha(x - x_0)$ with a minimum value of $-2\alpha^2$. This equation is related via Miura's transformation to Schrödinger's equation which has an eigenvalue of $\lambda = -\alpha^2$

(Problem 15.11)

Solitons, Schrödinger's Equation and Elementary Particles

In 1968, Miura found a remarkable connection between equation (15.11) and the equation

$$v_t + 6v^2v + v_{xxx} = 0 \quad (15.12)$$

which itself has a soliton solution.

Miura showed that if $v^2 + v_x = u$ then

$$\left(\frac{\partial}{\partial x} + 2v \right) (v_t - 6v^2v_x + v_{xxx}) = u_t - 6uu_x + u_{xxx} \quad (15.13)$$

(Problem 15.12)

So if v satisfies equation (15.12) with the sign of its second term changed, then u satisfies equation (15.11). Now Miura's transformation with

$$v^2 + v_x = u(x) \quad \text{and} \quad v = \psi_x / \psi$$

yields

$$\psi_{xx} - u(x)\psi = 0 \quad (15.14)$$

(Problem 15.13)

If $u(x)$ is now transformed to $u(x) - \lambda$, where λ is a constant, then equation (15.14) becomes Schrödinger's equation

$$\psi_{xx} + (\lambda - u(x))\psi = 0$$

with λ as an eigenvalue.

So Miura's transformation has related the KdV equation

$$u_t - 6uu_x + u_{xxx} = 0 \quad (15.11)$$

to Schrödinger's equation

$$\psi_{xx} + (\lambda - u(x)) \psi = 0 \quad (15.15)$$

Using the soliton solution

$$u = -2\alpha^2 \operatorname{sech}^2 \alpha(x - x_0)$$

of equation (15.11) we can show that the wave function

$$\psi = A \operatorname{sech} \alpha(x - x_0), \quad \text{where } A \text{ is a constant} \quad (15.16)$$

satisfies equation (15.15) when the eigenvalue $\lambda = -\alpha^2$ which is half the value of the minimum of the soliton with which it is associated (Figure 15.8) (See Gardner *et al.*, 1967).

(Problems 15.14, 15.15, 15.16)

Since λ is negative this represents a bound state in wave mechanics.

Other values of $\lambda > 0$ may be associated with solitons but these are not bound states and are related to progressive waves.

The fact that solitons may be associated with Schrödinger's equation and retain their unique identities in mutual collisions has led physicists to postulate that solitons may appear as massive elementary particles much heavier than the proton.

Solitons may enter particle physics in another way, confined not only in space but in time. In this case they are called instantons. Instantons have already been used to explain a pattern of particle masses which had posed a long-standing puzzle.

There are four ways of making quark–antiquark mesons from light quarks. Three of these mesons have been known for many years: the negative, positive and neutral pi mesons (pions) with masses equivalent to about 140 MeV (an electron equivalent mass is ~ 0.5 MeV).

The fourth meson has never been found but the eta meson has all the required properties except its mass which is about 550 MeV. Instantons explain this mass anomaly—they appear as energy excitations, located in space, in the field which binds the quarks together. They change the mass distribution among the mesons because they affect the various quark combinations in different ways (see Rebbi, 1979).

Optical Solitons

At the time of this writing the most practical use of solitons is in telecommunications. Optical fibres act as wave guides to microwaves and higher frequency electromagnetic waves and optical solitons are able to carry information along single mode silica fibres at multigigabit rates for distances greater than 9000 km, the width of the Pacific Ocean, with

a bit error rate (BER) $< 10^{-9}$, the international standard. Modern fibres have a very low loss rate of $< 1 \text{ dB km}^{-1}$ and an effective area of $\sim 30 \mu\text{m}^2$. The electrical power involved is very low and a total optical system is feasible including the amplifiers spaced along the cable. This permits a simpler, faster and more easily maintained system than that using conventional electronics. Research on optical solitons is world-wide but, for the English reader, the work of Linn Mollenauer and his colleagues at the A. T. & T. Bell Labs, New Jersey is the most accessible (see references).

Optical solitons have the normal sech^2 intensity profile and their amplitudes are given by sech wave function solutions to a non-linear Schrödinger equation (see Appendix, p. 555).

As with all solitons, optical solitons are produced by a balance between the competing effects of dispersion and non-linearity but the non-linearity of optical fibres is a very special case which contributes in a remarkable way to the maintenance of the soliton profile.

The Kerr Optical Effect and Self-phase Modulation In some materials, including silica fibres, the index of refraction for light of a given wavelength varies with the intensity of the light. This is the Kerr optical effect, which is expressed by

$$n - n_0 = n_2 I$$

where n is the index of refraction for a light wave of intensity I (large enough for non-linearity), n_0 is the refractive index for a low amplitude wave of the same frequency and n_2 is a constant equal to $3.2 \times 10^{-16} \text{ cm}^2 \text{ W}^{-1}$. The value of n_2 is small but the area of a single mode optical fibre $\sim 10^{-6} \text{ cm}^2$, so we must think in terms of megawatts per square metre. Moreover, the effects of non-linearity build up over fibre distances of many kilometres.

Since $n_2 I$ is positive we have

$$n - n_0 = c \left(\frac{1}{v} - \frac{1}{v_0} \right) > 0$$

so the phase velocity v of a high amplitude wave is less than v_0 , the phase velocity of a low amplitude linear wave of the same wavelength.

At a given wavelength this creates a phase retardation between the two amplitudes of

$$\Delta\phi = \frac{2\pi}{\lambda} L n_2 I$$

over a length L of the fibre. This phase retardation is obviously greater for the short wavelength high frequency components of the pulse, Figure 15.9, than for the lower frequencies and so in the high intensity central section of the pulse the higher frequencies are shifted towards the tail of the pulse while the lower frequencies advance to the front.

This process is opposed by the dispersive properties of the fibre because at the wavelength at which the solitons are centred; that is, $\lambda \sim 1.5 \mu\text{m}$ (1500 nm) the dispersion is negative (anomalous) so that $\partial v_g / \partial \lambda < 0$, where v_g is the group velocity.

Negative dispersion advances the trailing higher frequencies and retards the lower frequencies, both in a direction towards the centre of the pulse, so the pulse sharpens

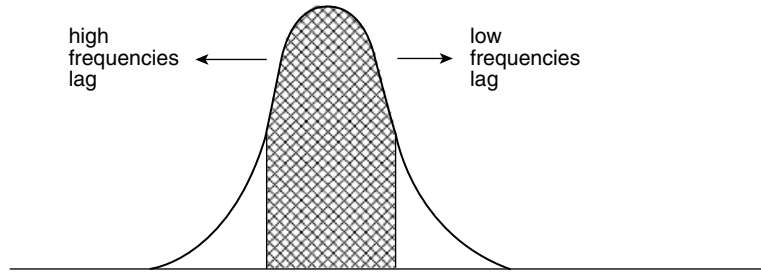


Figure 15.9 In the Kerr optical effect the velocity of light at a given wavelength depends upon its intensity. The high frequencies in the high intensity region of a soliton travelling in an optical fibre suffer a phase retardation; the low frequencies are advanced

towards a soliton sech^2 shape, Figure 15.10, and in a loss-free perfect silica fibre the soliton would maintain this shape indefinitely. In practice, the wavelength $\lambda \sim 1.5 \mu\text{m}$ is close to the minimum of the loss versus wavelength behaviour of the fibre, which accounts for low loss fibres of $< 1 \text{ dB km}^{-1}$. Optical amplifiers, which we shall discuss shortly, maintain the shape of the soliton over very long distances but even without amplification a soliton can travel several hundred kilometres along the fibre without changing its amplitude or shape.

This distance is called the soliton period, Figure 15.11, and is given by

$$z_0 = 0.322 \frac{\pi^2 c \tau^2}{\lambda_{\text{vac}}^2 D} = 0.39 \frac{\tau^2}{D} \quad \text{at } \lambda \sim 1.55 \mu\text{m}$$

where c is the velocity of light in free space, λ_{vac} is the wavelength in free space, τ is the full width at half the maximum value of the soliton and D is the group velocity dispersion parameter of the fibre; that is, the change in pulse delay with change in wavelength per unit of fibre length.

The units of τ are picoseconds and experimental solitons are produced in the range 1–50 ps. The units of D are picoseconds per nanometre per kilometre and experimental values of D are $\sim 10 \text{ ps nm}^{-1} \text{ km}^{-1}$. At $D \sim 1 \text{ ps nm}^{-1} \text{ km}^{-1}$ a 50 ps pulse has a soliton period $z_0 \approx 930 \text{ km}$.

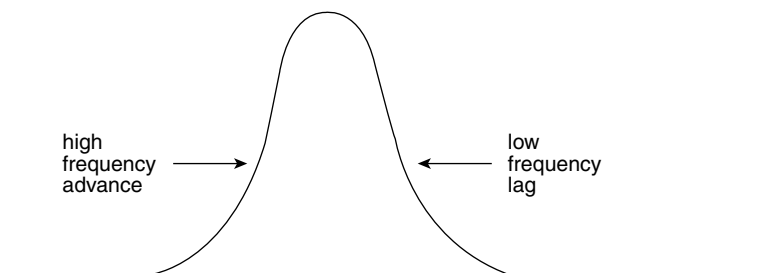


Figure 15.10 The effects of Figure 15.9 are reversed by the negative (anomalous) dispersion of the optical fibre at the wavelength on which the soliton is centred. This sharpens the soliton pulse

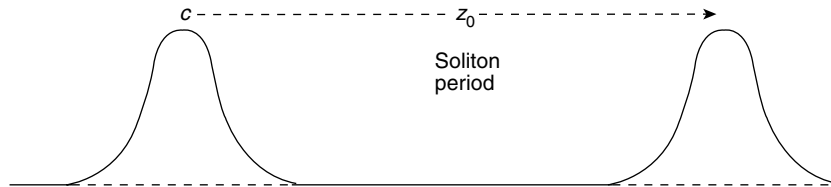


Figure 15.11 A soliton can travel several hundred kilometres in an optical fibre without being degraded in any way. This distance z_0 , is called the soliton period

Experimental Aspects Experimentally, the solitons are produced by a mode locked laser with an additional fibre arm in the feedback loop. As the laser builds up from noise the initially broad pulses are considerably narrowed by passing through the fibre arm and then reinjected back into the laser cavity, forcing the laser itself to produce narrower pulses. This process is repeated until the pulses become solitons and are ready for injection, via coupling, into the transmission system. The laboratory cable is a fibre spool ~ 75 km long and the solitons are recirculated through this loop to travel distances $> 10\,000$ km if required.

A typical laser soliton source produces pulses of ~ 50 ps with a power ~ 0.5 mW at a repetition rate of 2.5 GHz.

The Raman Effect This plays a very important role in optical soliton transmission. It arises when molecules in a material absorb radiation and it involves the vibrational and sometimes the rotational energy levels of the molecules. Figure 15.12 shows the vibrational

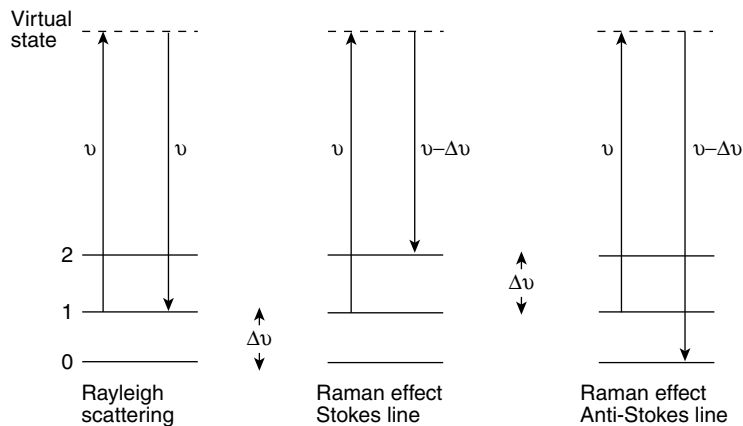


Figure 15.12 The Raman effect can degrade a soliton by transferring energy from its higher frequency to its lower frequency components. Vibrational energy levels in the optical fibre absorb higher frequency radiation ν from the soliton which reabsorbs it at a lower frequency $\nu - \Delta\nu$ (Stokes line). There are three possible processes. In Rayleigh scattering a photon returns to its original vibrational energy level, the Raman effect provides a frequency change $\Delta\nu = \pm 1$, where $\Delta\nu$ is the frequency interval between vibrational energy levels

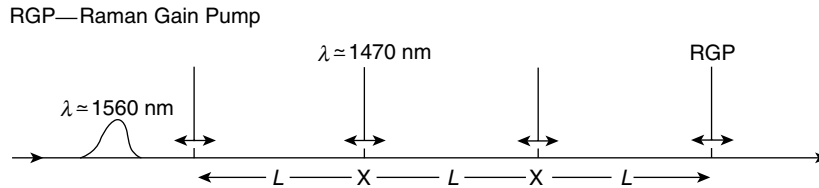


Figure 15.13 The transmission line acts as its own distributed amplifier when solitons accept higher energy photons via the Raman effect from optical pumps located at short intervals (distances $\ll z_0$, the soliton period). Excessive noise production is avoided by frequent low gain amplification (see Mollenauer *et al.*, 1986)

energy levels in a molecule with 0 as the ground state. Suppose initially that the molecule is in the energy level 1 and absorbs a photon of frequency ν which raises it to an excited level which may not be a stationary state. If the photon drops back to its original level the re-radiated photon of frequency ν is called Rayleigh scattering. However, selection rules also allow vibrational level changes $\Delta\nu = \pm 1$, where $\Delta\nu$ is the vibrational energy level interval, so the photon may drop back into level 2 or 0. The re-radiated or scattered photon will then appear at the frequencies $\nu - \Delta\nu$ (Stokes line) or $\nu + \Delta\nu$ (anti-Stokes line).

The Raman effect can ‘degrade’ a single soliton via a process known as the ‘self-frequency shift’. Here the vibrational levels of the silica fibre molecules absorb energy from the higher frequencies in the soliton pulse and the scattered radiation acts as a Raman pump for the lower frequencies in the pulse because the fibre provides a Raman acceptance band over a broad frequency spectrum.

Indeed, although a power of 0.5 mW provides a stable single soliton, early experiments showed that solitons with powers >1 W suffered from ‘self-frequency shift’ to such an extent that the soliton initially narrowed but then formed smaller satellite solitons.

The Raman Effect and Optical Amplification Solitons can gain energy via the Raman effect as well as lose it and this is the basis of amplification along an optical transmission line. One method results in the line acting as its own distributed amplifier. Laser pumps coupled into the line at regular intervals maintain the shape of a soliton by feeding in a frequency higher than that of the soliton, the energy difference being very close to the broad peak of the Raman gain band of the silica fibre. In Figure 15.13 the soliton wavelength is $\lambda = 1.5 \mu\text{m}$ and the lasers pump energy at $\lambda \approx 1.4 \mu\text{m}$. The pumps can also inject radiation in the counter-propagating direction, which helps to average out any effect of pump fluctuations; the penetration of the amplifying beam along the fibre is also enhanced. The intervals between the laser pumps are ~ 30 km which is a small fraction of the soliton period z_0 (\sim several hundred kilometres). In this way, the gain per interval is kept low enough to avoid excessive amplification of noise.

A second method, Figure 15.14 uses lumped amplifiers in the form of short lengths ~ 3 m of optically pumped fibres doped with a rare earth such as Erbium. Again, the interval between these lumped amplifiers is $\ll z_0$ the soliton period to keep the noise amplification low. The lumped amplifiers are energized by laser diode chips and for an input of ~ 10 mW a gain of 30–40 dB is obtained at the useful wavelengths. The power of

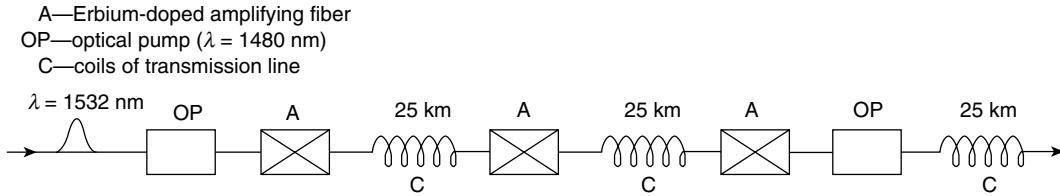


Figure 15.14 Solitons are now maintained by lumped amplifiers in the form of $\approx 3 \text{ m}$ lengths of optically pumped fibres doped with the rare earth Erbium separating 25 km lengths of transmission line. The interval between the low gain amplifiers $\ll z_0$ (the soliton period) to avoid noise amplification

these amplifiers is useful in multiplexing, the subject of the next section (see Desurvire, 1992).

Multiplexing This refers to the possibility of sending more than one channel of information down a single fibre. In current transmission systems, non-linear interaction causes severe interchannel interference but solitons are transparent to each other. They are unaffected by collisions and do not interfere with each other.

In multiplexing, two channels along a single fibre are provided by solitons which are polarized in planes perpendicular to each other.

Even more channels are possible with wavelength division multiplexing. Solitons of different wavelengths have different velocities and analysis shows that in a system using a chain of lumped amplifiers, adjacent WDM (wavelength division multiplexed) solitons interact just as in a lossless fibre so long as the collision length (twice the length of a soliton) is two or three times the amplifier spacing (Figure 15.15).

This implies that several multigigabit per second WDM channels spanning a wavelength separation of 1 or 2 nm may be used in a single fibre.

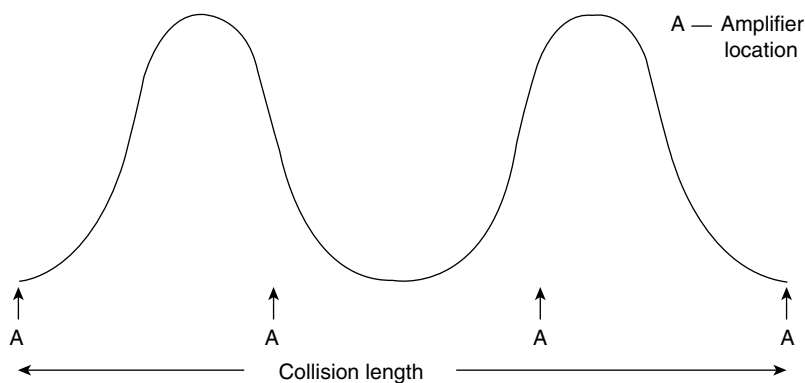


Figure 15.15 Wavelength division multiplexing is possible with solitons of different wavelengths and velocities. These solitons do not interfere with each other so long as the collision length (twice a soliton length) is two or three times the lumped amplifier spacing (see Mollenauer *et al.*, 1990)

In a conventional transmission line each channel must be isolated at the regenerative amplifiers and separately processed but one amplifier can handle all soliton channels and Erbium-doped amplifiers are powerful enough to do this.

Random Noise Effects and the Frequency Sliding Guiding Filter There are two main sources of error which affect an optical soliton transmission system: fluctuations of pulse energy and arrival time at the receiver. Spontaneous emission (noise) always accompanies coherent Raman gain and at each amplifier, amplified spontaneous emission (ASE noise) is added to a soliton which can change its energy and its central frequency in a random way. The change of energy may affect the amplitude of a soliton and the accumulated effect may reduce a soliton to such an extent that its intended arrival as a ONE in the bit system is registered as a ZERO. Alternatively, amplified noise may register a ONE in a ZERO space. This contributes to the bit error rate (BER) which must be kept below the international standard of $< 10^{-9}$.

The ASE change in the frequency of the soliton changes its velocity and therefore affects its arrival time, throwing the pulse out of its proper time slot.

Amplitude and time jitter may be reduced by narrowing the bandwidth of the transmission line (Mollenauer, 1994), using a narrow band filter at each amplifier. Each filter is a low-finesse Fabry–Perot etalon (p. 343), centred on the true frequency peak of the soliton (Figure 15.16). A soliton whose frequency has been shifted from the filter peak suffers a loss across the spectrum provided by the filter. This, together with the non-linear effect which generates new frequencies, pushes the soliton back towards the filter peak. In this way, the noise-induced frequency shift is returned to zero rather than being maintained as it would in a broad-band transmission line.

Amplitude jitter is damped because a pulse with excess energy will narrow in time and broaden in spectrum more than the average and will suffer a greater loss at each filter. However, the soliton loss at each filter must be replaced at each amplifier by an excess gain with a resulting growth in noise.

Mollenauer *et al.* (1994), found that even when the soliton source laser was not tuned exactly to the filter peak frequency, the soliton was still guided rapidly on to the filter peak. The filter peak frequencies were therefore gradually slid with distance so that the soliton frequency followed the filters while the noise remained in its original frequency band and

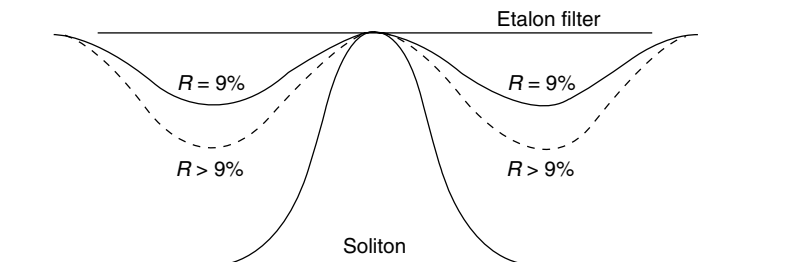


Figure 15.16 Noise effects in an optical transmission line are reduced using a narrow band Fabry–Perot etalon filter at each amplifier. The low finesse, $R \sim 9\%$, of fixed frequency filters can be increased, $R > 9\%$, if the frequency of the filters is gradually shifted with distance along the line. The soliton frequency has no difficulty in adjusting itself to this shift and noise is progressively reduced (see Mollenauer *et al.*, 1994)

its growth was inhibited. This noise reduction allowed the etalon filters to be strengthened to a higher finesse. Experiments with a soliton pulse width of $\tau \sim 16$ ps, $D \sim 0.5$ ps nm⁻¹ km⁻¹, amplifier spacing = 26 km with one filter per amplifier, and a frequency sliding rate of 7 GHz 10⁻³ km gave a net frequency shift over 9000 km (trans-Pacific distance) of a few soliton bandwidths, i.e. 0.5 nm at $\lambda = 1557$ nm. Such a series of sliding frequency etalon filters can operate over a range of wavelengths wide enough to allow several channels of wavelength division multiplexing.

Problem 15.1

The properties of a stationary gas at temperature T_0 in a large reservoir are defined by c_0 , the velocity of sound, $h_0 = c_p T_0$, the enthalpy per unit mass, and γ , the constant value of the specific heat ratio. If a ruptured diaphragm allows the gas to flow along a tube with velocity u , use the equation of conservation of energy to prove that

$$\frac{c_0^2}{\gamma - 1} = \frac{\gamma + 1}{2(\gamma - 1)} c^{*2}$$

where c^* is the velocity at which the flow velocity equals the local sound velocity.

Hence show that if $u_1/c^* = M^*$ and $u_1/c_1 = M_s$, then

$$M^{*2} = \frac{(\gamma + 1)M_s^2}{(\gamma - 1)M_s^2 + 2}$$

Problem 15.2

Using a coordinate system which moves with a shock front of velocity u_1 , show from the conservation equations that c^* in Problem 15.1 is given by

$$c^{*2} = u_1 u_2$$

where u_2 is the relative flow velocity behind the shock front.

Problem 15.3

Use the conservation equations to prove that the pressure ratio across a shock front in a gas of constant γ is given by

$$\frac{p_2}{p_1} = \frac{\beta - \alpha}{1 - \beta\alpha}$$

where $\beta = \rho_2/\rho_1$, the density ratio, and $\alpha = (\gamma - 1)/(\gamma + 1)$.

Problem 15.4

Use the results of Problems 15.1 and 15.2 with the equation of momentum conservation to prove that the shock front Mach number is given by

$$M_s = \frac{u_1}{c_1} = \sqrt{\frac{y + \alpha}{1 + \alpha}}$$

where $y = p_2/p_1$, the pressure ratio across the shock and $\alpha = (\gamma - 1)/(\gamma + 1)$. Hence show that the flow velocity behind the shock is given by

$$u = \frac{c_1(1 - \alpha)(y - 1)}{\sqrt{1(1 + \alpha)(y + \alpha)}}$$

Problem 15.5

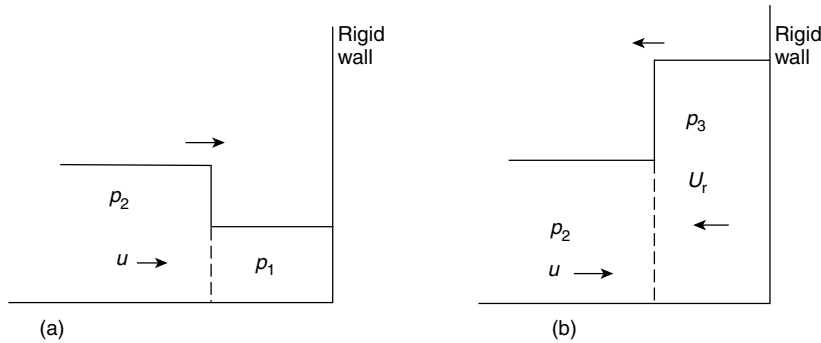
The diagrams show (a) a shock wave of pressure p_2 and flow velocity u propagating into a stationary gas, pressure p_1 , and (b) after reflexion at a rigid wall the reflected wave of pressure p_3 moving back into the gas behind the incident shock still at pressure p_2 . Use the result at the end of Problem 15.4 to show that the flow velocity u_r behind the reflected wave is given by

$$\frac{u_r}{c_2} = \frac{(1 - \alpha)(p_3/p_2 - 1)}{\sqrt{(1 + \alpha)(p_3/p_2 + \alpha)}}$$

and since $u + u_r = 0$ at the rigid wall, use this result together with the ratio for $c_2/c_1 = (T_2/T_1)^{1/2}$ to prove that

$$\frac{p_3}{p_2} = \frac{(2\alpha + 1)y - \alpha}{\alpha y + 1}$$

where $y = p_2/p_1$ and $\alpha = (\gamma - 1)/(\gamma + 1)$.



Problem 15.6

Use Problem 15.5 to prove that the ratio

$$\frac{p_3 - p_1}{p_2 - p_1} \rightarrow 2 + \frac{1}{\alpha}$$

in the limit of very strong shocks. (Note that this value is 8 for $\gamma = 1.4$ and 6 for $\gamma = 5/3$, compared with the normal acoustic pressure jump of 2 upon reflexion.)

Problem 15.7

Equation (15.9) evaluates u_x for $u = f(x - ut)$. Obtain u_t in a similar way and use this with equation (15.9) to prove equation (15.8).

Problem 15.8

Burger's equation $u_t + uu_x - \nu u_{xx} = 0$ where $\nu > 0$ is a special case. It has a second-order dispersion term and is directly integrable. Show that $u = -2\nu\psi_x/\psi$ transforms Burger's equation into the diffusion equation

$$\frac{\partial^2 \psi}{\partial t^2} = \nu \frac{\partial^2 \psi}{\partial x^2}$$

For fluids, ν is a measure of viscosity which dissipates excess momentum in non-linear waves.

Problem 15.9

Show that $u(x, t) = 2\alpha^2 \operatorname{sech}^2 \alpha(x - ct)$ is a soliton solution of the KdV equation $u_t + 6uu_x + u_{xxx} = 0$ after calculating u_t, u_x and u_{xxx} as shown in the text.

Problem 15.10

For small values of q , $\log(1 + q) \approx q$. Show that values of $u(x, t)$ near the base of Figure 15.5(a) where $uu_x \approx 0$ may be written

$$u(x, t) \approx 2 \frac{\partial^2}{\partial x^2} e^{-2\alpha(x-ct)}$$

and that this satisfies the dispersion equation $u_t + u_{xxx} = 0$ if $c = 4\alpha^2$.

Problem 15.11

Use the method of Problem 15.9 to show that $u(x) = -2\alpha^2 \operatorname{sech}^2 \alpha(x - x_0)$ is a solution of the KdV equation $u_t - 6uu_x + u_{xxx} = 0$.

Problem 15.12

Prove equation (15.13) if $u = v^2 + v_x$.

Problem 15.13

Verify equation (15.14) for $u(x) = v_x + v^2$ and $v = \psi_x/\psi$.

Problem 15.14

Show that the wave function $\psi = A \operatorname{sech} \alpha(x - x_0)$ where A is a constant satisfies Schrödinger's equation (15.15) when $\lambda = -\alpha^2$.

Problem 15.15

KdV equations are invariant to a Galilean transformation. Show that the transformations $u \rightarrow u - \lambda$ where λ is constant together with $x \rightarrow x + 6\lambda t$ returns $u_t + 6uu_x + u_{xxx} = 0$ to its original form.

Problem 15.16

At time $t = 0$ a high amplitude signal has a profile $y = a \sin \pi x$ with $\partial y/\partial t = 0$. Thereafter, it propagates according to the non-linear wave equation

$$\frac{\partial^2 y}{\partial t^2} = c_0^2 \left(1 + \varepsilon \frac{\partial y}{\partial x} \right) \frac{\partial^2 y}{\partial x^2}$$

where ε is a small positive constant.

Show that the time required for the leading edge of a positive signal to become infinitely steep is given by

$$t = 4/c_0 \varepsilon a \pi^2$$

Hint: Rayleigh's method (Rayleigh, *Theory of Sound*, Vol. 2, Dover Press p. 35), shows the required time to be the reciprocal of the maximum value of $|du/dx|$ where du is the relative phase velocity between two points on the leading edge of a positive signal separated by a horizontal distance dx . Note that waves propagate in the positive and negative x -directions.

Bibliography

- Solitons and Non-Linear Wave Equations* by Dodd, K. R. *et al.* Academic Press, New York (1983).
Non Linear Waves, Solitons and Chaos by Infeld, E. and Rowlands, G., Cambridge University Press, Cambridge (1990).
Waves Called Solitons, Concepts and Experiments by Remoissenet, M., Springer Verlag, Berlin (1994).
Non-Linear Physics, Vol. 4, Contemporary Concepts in Physics by Sagdeev, R. Z., Usikov, D. A. and Zaslavsky G. H., Harwood Academic Press, Chur, Switzerland (1990).
Non-Linear Waves and Solitons by Toda, M., Kluwer Academic Publishers, Dordrecht (1989).

References

- Desurvire, E. (1992), *Scientific American* (January).
 Gardner, C. S., Greene, J. M., Kruskal, M. D. and Miura, R. (1967), *Phys. Rev. Lett.*, **19**, 1095.
 Korteweg, D. J. and de Vries, G. (1895), *Phil. Mag.*, **39**, 422.
 Miura, R. (1968), *J. Math. Phys.*, **9**, 1202.
 Rayleigh, Lord, (1876), *Phil. Mag.*, (5), 1, 257.
 Rebbi, C. (1979), *Scientific American* (February).
 Sagdeev, R. Z. and Kennel, C. F. (1991), *Scientific American* (April).
 Scott–Russel, J. (1844), *Proc. Roy. Soc. Edinburgh*, 319.
 Zabusky, N. and Kruskal, M. D. (1965), *Phys. Rev. Lett.*, **15**, 240.

Selected references in chronological order from:

- Mollenauer L. *et al.*: *Phys. Rev. Lett.*, **45**, 1095 (1980).
Fibreoptic Technology, April (1982).
Optics Lett., **9**, 13 (1984).
Phil. Trans. Royal Soc., London, **A 315**, 437 (1985).
Optic News, **12**, 42 (1986).
J. I. E. E., Journal of Quantum Electronics, **22**, 157 (1986).
Optics Lett., **13**, 675 (1988).
Phys. World, 29, September (1984).
Optics Lett., **15**, 1203 (1990).
J. Lightwave Technol., **9**, 3 (1991).
Laser Focus World, 159, November (1991).
Optics Lett., **17**, 1575 (1992).
Optics and Photonic News, **15**, April (1994).

